Enhanced cooperative navigation by data fusion from IMU, ambiguous terrain navigation, and coarse relative states

Merlinge, N. J. A., Brusey, J., Horri, N., Dahia, K. & Piet-Lahanier, H.

DOI 10.1109/CDC.2017.8263693

Publisher: IEEE

Enhanced cooperative navigation by data fusion from IMU, ambiguous terrain navigation, and coarse relative states

Nicolas Merlinge, James Brusey, Nadjim Horri, Karim Dahia, Hélène Piet-Lahanier

***Abstract*— GNSS denied IMU correction is a practical challenge in aerospace vehicle navigation. In the context of several vehicles flying in formation, navigation accuracy can be enhanced by communication between the vehicles. In this paper, a collaborative navigation strategy is presented to deal with coarse and ambiguous measurements. An absolute navigation filter provides a first estimate of the navigation solution, while a relative observer rebuilds the neighbors relative states from embedded seekers. A high-level Master Filter fuses information provided by those two low-level filters to enhance the navigation solution. Absolute navigation measurements are terrain elevation data correlated with a Digital Elevation Model map. Since they are highly ambiguous and nonlinear, they are processed by a Box Regularized Particle Filter. The relative measurements under consideration suffer a high level of uncertainty, especially on the relative distance between vehicles. By fusing all uncertain data, a complete and accurate navigation solution is obtained. Numerical results are presented and show an enhancement in navigation performance by exchanging information, in terms of RMS estimation error (63% more accurate in position), estimation confidence (78% more precise in position), and computational load (requires 83% less operations).**

I. INTRODUCTION

Autonomous aircraft formation flying is an active research area (e.g., Wu [1]), but often requires accurate absolute navigation. Aircraft navigation systems rely on an Inertial Measurement Unit (IMU) to estimate their position and attitude. Given that this IMU uses an iterative scheme of acceleration integration, it drifts and needs to be corrected using additional measurements. In order to be independent from any external navigation systems that can be jammed or disturbed, e.g., Global Navigation Satellite System (GNSS), more autonomous sensors can be used, such as optical seekers or electromagnetic sensors.

A possible approach is terrain navigation, i.e. measurements of the ground relative elevation combined with an embedded Digital Elevation Model (DEM) map. However, such measurements are highly nonlinear and ambiguous due to terrain similarities, and cannot be efficiently processed by classic methods such as Kalman Filters. Multi-hypothesis filtering methods, such as Particle Filters, are proven to be able to handle this issue (e.g., Dahia [2]). Nevertheless, they often suffer from low robustness to terrain ambiguities and are complex to compute. More recently, an interval analysis based particle filter has been proposed, called Box Regularized Particle Filter (BRPF, Merlinge [3]). Taking advantage of both studies on interval-based particle filters (e.g., Gning [4]) and probabilistic kernel estimation (e.g., Musso [5]), the BRPF offers a high robustness to terrain ambiguities. However, it may converge slowly and its estimated confidence often remains too pessimistic for accurate formation flying. A possible solution is to take advantage of the other vehicles to make the estimator converge faster with a reduced estimated uncertainty by observing the vehicle's neighbors' relative states and by receiving information about their own navigation estimate.

An observability study was presented in Sharma [6] showing that the IMU drift can be constrained using inter-vehicle coarse absolute state communications fused with relative measurements. The simplest way to fuse those measurements is a single layer architecture made of one global navigation filter (e.g., [6], [7]). However, this architecture cannot guarantee that a given combination of relative measurements will not make the estimate navigation accuracy deteriorate. Furthermore, the computation load of the fusion algorithm can be high, as shown later in the article for a BRPF. To achieve a robust decentralized architecture, two layers architectures have been proposed (e.g., [8], [9]), inspired by the theoretical work of Carlson [10]. In those approaches, absolute IMU correction and relative observations are tackled separately in a first layer and then fused with the communicated states in a second layer.

In this paper, a two stages decentralized navigation architecture is proposed to refine robust terrain navigation performed by a Box Regularized Particle Filter by exchanging states between vehicles. The practical value of the approach is shown through a computation load complexity analysis and numerical simulations.

The article is organized as follows. Section II presents the terrain navigation based IMU correction scheme and the relative tracking model. Section III presents a cooperative navigation enhancement strategy and compare it with a single layer architecture. Numerical results are presented in Section IV.

II. PROBLEM STATEMENT

We consider a fleet of N UAVs flying in formation. The state vector $\mathbf{X}^i$ of each vehicle $i \in [\![1, N]\!]$ consists of:

$$\mathbf{X}^i = \left[\mathbf{p}^{iT}, \mathbf{V}^{iT}, \boldsymbol{\psi}^{iT}\right]^T \in \mathbb{R}^9 \tag{1}$$

where $\mathbf{p}^i = \left[p^i_\lambda, p^i_\phi, p^i_h\right]^T$ is the geographical position (respectively latitude, longitude, altitude), $\mathbf{V}^i \in \mathbb{R}^3$ is the velocity vector, and $\boldsymbol{\psi}^i \in \mathbb{R}^3$ is the attitude. The IMU provides

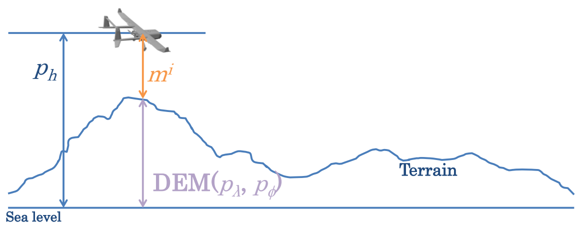

Fig. 1. Elevation measurement m^i in terrain navigation

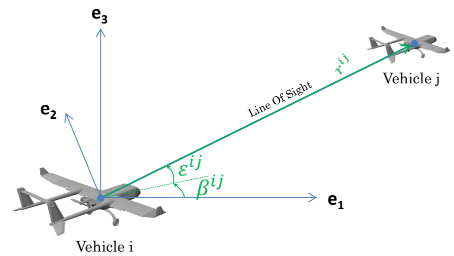

Fig. 2. Relative measurements $(\beta^{ij}, \varepsilon^{ij}, r^{ij})$

position, velocity, and attitude information in Earth fixed reference frame by integrating the measured accelerations and angular rates. The inertial observations are expressed as:

$$\tilde{\mathbf{X}}^i = \left[\tilde{\mathbf{p}^i}^T, \tilde{\mathbf{V}^i}^T, \tilde{\boldsymbol{\psi}^i}^T, \tilde{\boldsymbol{\Gamma}^i}^T, \tilde{\boldsymbol{\Omega}^i}^T\right]^T \in \mathbb{R}^{15} \tag{2}$$

where $\tilde{\boldsymbol{\Gamma}}^i \in \mathbb{R}^3$ is the measured acceleration and $\tilde{\boldsymbol{\Omega}}^i \in \mathbb{R}^3$ is the measured angular rate. However, IMU measurements suffer uncertainty that results in a growing drift.

A. IMU correction by ground altitude measurements

1) Dynamical model: inertial error: The IMU errors can be modeled as a state vector $\mathbf{X}^i_{err}$ defined by:

$$\mathbf{X}^i_{err} = \left[\boldsymbol{\delta}\mathbf{X}^{i^T}, \boldsymbol{\delta}\mathbf{V}^{i^T}, \boldsymbol{\delta\psi}^{i^T}, {\mathbf{b}^i_a}^T, {\mathbf{b}^i_g}^T\right]^T \in \mathbb{R}^{15} \tag{3}$$

where $\boldsymbol{\delta}\mathbf{X}^i$ is the position error converted in m, and $\boldsymbol{\delta}\mathbf{V}^{i^T}$, $\boldsymbol{\delta\psi}^{i^T}$, ${\mathbf{b}^i_a}^T$, ${\mathbf{b}^i_g}^T$ are respectively the inertial error on velocity, attitude, and the accelerometers and gyrometers bias. Estimating the IMU errors $\mathbf{X}^i_{err}$ by using additional sensors (e.g., GNSS, Radar-altimeter) makes it possible to correct the inertial measurements $\tilde{\mathbf{X}}^i$. The inertial error evolution can be described by the following dynamical model:

$$\dot{\mathbf{X}}^i_{err} = \mathbf{A}^i\mathbf{X}^i_{err} + \mathbf{w}^i \tag{4}$$

where $\mathbf{A}^i \in \mathbb{R}^{15\times 15}$ is the transition matrix coupling the dynamics of inertial error and $\mathbf{w}^i \in \mathbb{R}^{15}$ a process noise quantifying the dynamical model uncertainty. Dahia [2] provides a complete derivation of inertial equations and inertial error.

2) Observation model: ground altitude measurements: A radar altimeter provides elevation measurements (the relative height m^i, see Fig. 1) along the aircraft trajectory at discrete time values. By comparing onboard elevation measurements with a Digital Elevation Model ($DEM : \mathbb{R}^2 \to \mathbb{R}$), it is possible to reconstruct the absolute position of the aircraft. The DEM gives the absolute elevation as a function of the geographical coordinates (p^i_λ, p^i_ϕ). The measurement equation is:

$$m^i = g(\mathbf{X}^i) + v \tag{5}$$

where $v \in \mathbb{R}$ is the measurement noise modeling the sensor error and the DEM map uncertainty, and

$$g(\mathbf{X}^i) = p^i_h - DEM(p^i_\lambda, p^i_\phi) \tag{6}$$

is the observation function. There is no analytic description of g, since DEM is obtained from an embedded terrain map.

B. Relative state observation

In order to use navigation information from other vehicles, each vehicle needs to estimate the relative state for each neighbor, based on measuring its relative position.

1) Relative dynamical model: Let $\mathbf{X}^{ij}$ be the relative state vector between the current vehicle i and vehicle j:

$$\mathbf{X}^{ij} = \left[x^{ij}, y^{ij}, z^{ij}, V^{ij}_x, V^{ij}_y, V^{ij}_z\right]^T \tag{7}$$

where x, y , and z denote the three axis of a relative frame aligned on the absolute one and centered to the vehicle. V_x, V_y, and V_z are the associated velocities. The relative dynamical evolution can be written as:

$$\dot{\mathbf{X}}^{ij} = \boldsymbol{\Phi}\mathbf{X}^{ij} + \mathbf{B}\left(\boldsymbol{\Gamma}^j - \boldsymbol{\Gamma}^i\right) + \mathbf{w}^{ij} \tag{8}$$

with $\boldsymbol{\Phi} = \begin{bmatrix} \mathbf{I}_3 & \mathbf{0}_{3\times3} \\ \mathbf{0}_{3\times3} & \mathbf{0}_{3\times3} \end{bmatrix}$. $\mathbf{I}_d$ and $\mathbf{0}_{d\times d}$ are respectively the identity matrix and the zero matrix of dimension d. The current vehicle acceleration can be provided by the IMU corrected by the navigation filter. Neighbor j acceleration $\boldsymbol{\Gamma}^j$ is assumed to be communicated every Δt_{com}. Since the communication frequency may be lower than the relative system dynamics, this acceleration may suffer uncertainty, modeled by an additive noise $\mathbf{w}^{ij} \in \mathbb{R}^6$.

2) Relative observation model: The measurements consist of the bearing β^{ij} and elevation ε^{ij} angles, and the relative range r^{ij}, which can be expressed as $\mathbf{m}^{ij} = h\left(\mathbf{X}^{ij}\right) + \mathbf{v}_r$. with $\mathbf{v}_r \in \mathbb{R}^3$ the observation uncertainty and

$$h\left(\mathbf{X}^{ij}\right) = \begin{bmatrix} \beta^{ij} \\ \varepsilon^{ij} \\ r^{ij} \end{bmatrix} = \begin{bmatrix} \text{atan2}\left(y^{ij}, x^{ij}\right) \\ \text{atan2}\left(z, \sqrt{{x^{ij}}^2 + {y^{ij}}^2}\right) \\ \sqrt{{x^{ij}}^2 + {y^{ij}}^2 + {z^{ij}}^2} \end{bmatrix} \tag{9}$$

Measurements are illustrated in Figure 2. In the case of passive embedded relative sensors, the range is usually obtained with a low accuracy and a low update rate, which results in a highly uncertain relative estimate. The next section presents a two-layers data fusion architecture that is robust to large estimation uncertainty while reducing the computational load with respect to a single layer architecture.

III. PROPOSED FUSION ARCHITECTURE

In this section, a fusion architecture is described. It consists of two levels. The first level is composed of two

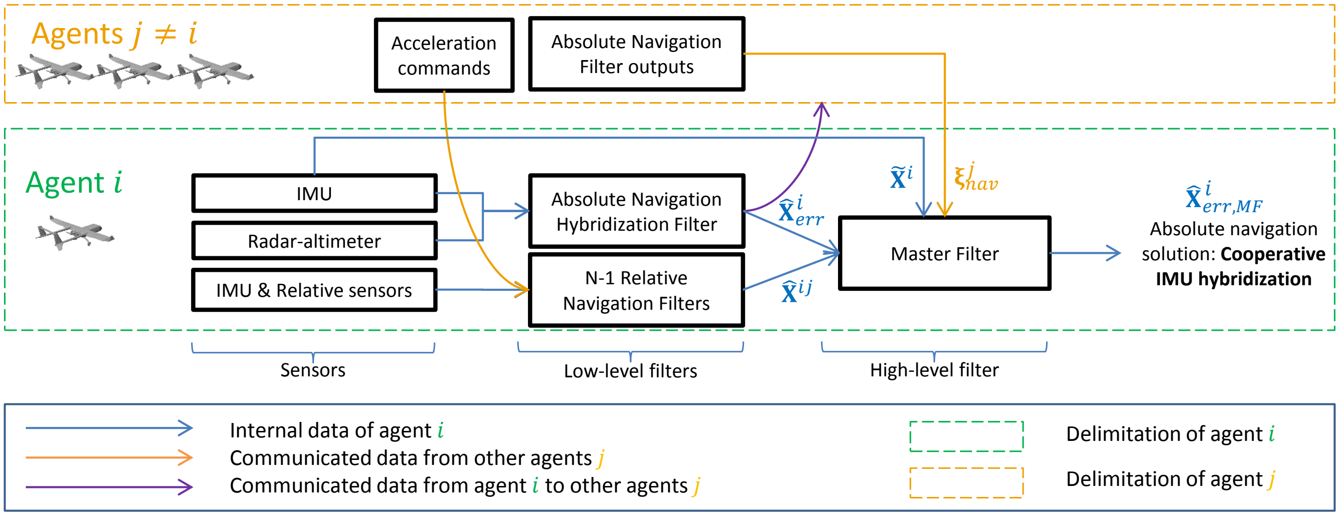

Fig. 3. Proposed two layers fusion architecture

parallel low-level filters processing absolute navigation measurements on the one hand and relative measurements on the other hand. For absolute navigation, a Box Regularized Particle Filter (BRPF) provides a first version of the navigation solution (IMU error estimation from radar-altimeter measurements). For relative navigation, an EKF rebuilds the relative states between neighbors j and vehicle i. Then, a high-level filter, called Master Filter in what follows, fuses the low-level filters' output with communicated low-level navigation solutions from other vehicles.

A. Absolute and relative navigation filters

To correlate terrain elevation measurement with a DEM map, a Box Regularized Particle Filter has been proposed by Merlinge [3] and is briefly described here. In what follows, k denotes a discrete time. The BRPF defines a cloud of Box Particles $[\mathbf{X}_k^i] \in \mathbb{IR}^d$ (with $\mathbb{IR}$ the interval set on $\mathbb{R}$ and d the state dimensionality.). In this section, i denotes the index of each particle. Each Box Particle is associated with a weight w_k^i that quantifies its likelihood to contain the real state $\mathbf{X}_{err}$ (inertial error vector) to be estimated. This likelihood is computed from the current measurements box $[\mathbf{m}_k]$ constructed as a confidence interval around the sensor value. No additional probabilistic hypothesis about the measurement uncertainty is needed excepted its support.

Figure 4 describes the algorithm. Matrix $\mathbf{F}_A$ is the discretized form of $\mathbf{A}$ in (4). A box $[\mathbf{a}] \in \mathbb{IR}^d$ is defined as a d-dimensional vector of intervals. In what follows, $\mathbf{C}_k^i \in \mathbb{R}^d$ stands for the i^{th} box particle center. The volume of a box $|[\mathbf{a}]| \in \mathbb{R}$ is defined as the product of the length of each interval. An extensive description of interval analysis is available in [11]. An associated empirical covariance $\widehat{\mathbf{P}}_{nav,k} \in \mathbb{R}^{d\times d}$ can be computed to quantify the estimate confidence. The whole number of elementary operations (addition, substractions, multiplications, divisions) performed during one iteration of the algorithm described in figure 4 has been evaluated using the same methodology as in [12]:

$$c_{BRPF}(d, N_p) = N_p(12d^2 + 2d + 1) \qquad (10)$$

Initialization ($k = 1$): Generate N_p box particles $\{[\mathbf{X}_k^i]\}_{i\in[\![1,N_p]\!]}$
for each time-step $k = 1$ to k_{end} **do**
  for each particle $i = 1$ to N **do**
    Prediction: $[\mathbf{X}^i_{k|k-1}] = \mathbf{F}_A[\mathbf{X}^i_{k-1}] + [\mathbf{w}_k]$
    Correction:
    • Box contraction: find the smallest box $[\mathbf{X}^i_{k|k}]$ that contains $\{\mathbf{S}_k^i\} = \left\{\mathbf{X}_k \in [\mathbf{X}^i_{k|k-1}] | g(\mathbf{X}_k) \in [\mathbf{m}_k]\right\}$
    • Likelihood: $\lambda_i = \frac{|[\mathbf{X}^i_{k|k}]|}{|[\mathbf{X}^i_{k|k-1}]|}$
    • Weight update: $w_k^i = w_{k-1}^i \lambda_i$
    • Weight normalization: $w_k^i \leftarrow \frac{w_k^i}{\sum_{j=1}^N w_k^j}$
    if $1/\sum_{i=1}^{N_p} {w_k^i}^2 < \theta_{eff} N_p$ with $\theta_{eff} \in [0, 1]$ **then**
      Resampling by subdivision:
      resample to create N_p new particle boxes with weights equal to $1/N_p$. Perform a kernel regularization (see Merlinge [3])
    end if
    State estimation:
    • Estimate: $\widehat{\mathbf{X}}_{err,k} = \sum_{i=1}^{N_p} w_k^i \mathbf{C}_k^i$ and confidence: $\widehat{\mathbf{P}}_{nav,k}$
  end for
end for

Fig. 4. Box Regularized Particle Filter algorithm

When GNSS is unavailable, this algorithm makes it possible to solve the navigation problem with high robustness to terrain ambiguities, but converges slowly and may remain pessimistic. For relative navigation, the dynamical model (8) is linear, and measurements (9) are somewhat nonlinear. Thus, an Extended Kalman Filter (EKF) is an efficient solution. The relative estimate is denoted $\widehat{\mathbf{X}}^{ij} \in \mathbb{R}^6$ and associated to covariance confidence $\widehat{\mathbf{P}}^{ij} \in \mathbb{R}^{6\times 6}$.

B. Master filter

The Master Filter fuses current vehicle filters' output with communicated information from neighbors. In what follows, i denotes the current vehicle index and $j \neq i$ denote its neighbors.

1) Communication strategy: A vehicle cannot emit and receive data at the same time. Therefore, communication is constrained by this condition. As proposed in Leung [13], an *a priori* communication order has been defined for the communication period Δt_{com}. Each vehicle has a time range

Fig. 5. Communication protocol

$\frac{\Delta t_{com}}{N}$ to send its data to others. This communication protocol is illustrated in Figure 5. The assumption is made that all vehicles are time-synchronized. The hypothesis is made that the communication graph is fully connected and that received data are immediately available. Vehicle j sends its estimated absolute position and velocity, its acceleration, and their associated uncertainties. The communicated absolute state and its uncertainty are respectively denoted $\boldsymbol{\xi}^i_{nav} \in \mathbb{R}^6$, and $\mathbf{R}^i_{nav} \in \mathbb{R}^{6\times 6}$. Information flow is illustrated in Figure 3.

2) Master Filter: Each time the current vehicle receives $\boldsymbol{\xi}^i_{nav}$ and $\mathbf{R}^i_{nav}$, it can translate them in terms of its own position and velocity through its relative navigation solution $\widehat{\mathbf{X}}^{ij}$. This pseudo-measurement $\boldsymbol{\xi}^{i|j} \in \mathbb{R}^6$ of state i given state j is defined as:

$$\boldsymbol{\xi}^{i|j} = \boldsymbol{\xi}^j_{nav} - \mathbf{G}_{geo}\widehat{\mathbf{X}}^{ij} \tag{11}$$

where $\mathbf{G}_{geo}$ transforms metric distance to angular geographic difference. The associated uncertainty is, under the hypothesis of $\boldsymbol{\xi}^j_{nav}$ and $\widehat{\mathbf{X}}^{ij}$ being statistically independent:

$$\mathbf{R}^{i|j} = \mathbf{R}^i_{nav} + \widehat{\mathbf{P}}^{ij} \tag{12}$$

The geographic state $\boldsymbol{\xi}^{i|j}$ must be converted to inertial error with respect to the current vehicle IMU data $\tilde{\mathbf{X}}^i$: $\boldsymbol{\xi}^{i|j}_{err} = \mathbf{G}_m\left(\boldsymbol{\xi}^{i|j} - \mathbf{H}\tilde{\mathbf{X}}^i\right)$ where $\mathbf{G}_m$ transforms angular geographic difference to metric distance and $\mathbf{H} = \begin{bmatrix}\mathbf{I}_6 & \mathbf{0}_{6\times 9}\end{bmatrix}$. As stated in III-A, the navigation filter provides a first estimate of IMU errors $\widehat{\mathbf{X}}_{err} \in \mathbb{R}^d$. The IMU error model has a linear formulation and the relationships between $\boldsymbol{\xi}^j_{nav}$, $\widehat{\mathbf{X}}^{ij}$, and $\widehat{\mathbf{X}}_{err}$ are linear. This is a sufficient condition for the iterative least square estimator to be minimum variance (Oudjane [14]). It is known as the Information Filter, in other words the information formulation of the Kalman Filter (Grocholsky [15]). The Master Filter output is thus:

$$\widehat{\mathbf{X}}^i_{err,k,MF} = \widehat{\mathbf{P}}^i_{k,MF}\left(\widehat{\mathbf{P}}^{i}_{k|k-1,MF}{}^{-1}\widehat{\mathbf{X}}^i_{err,k|k-1,MF} + \mathbf{i}^i_k\right) \tag{13}$$

with

$$\widehat{\mathbf{X}}^i_{err,k|k-1,MF} = \mathbf{F}_A\widehat{\mathbf{X}}^i_{err,k-1,MF} \tag{14}$$

$$\widehat{\mathbf{P}}^i_{k|k-1,MF} = \mathbf{F}_A\widehat{\mathbf{P}}^i_{k-1,MF}\mathbf{F}_A^T + \mathbf{Q}_{MF} \tag{15}$$

where $\mathbf{F}_A$ is the discretized transition matrix defined in II-A and $\mathbf{Q}_{MF} \in \mathbb{R}^{15\times 15}$ the process covariance uncertainty, $\mathbf{i}^i_k = \mathbf{H}^T\widehat{\mathbf{P}}^i_{nav,k}{}^{-1}\widehat{\mathbf{X}}^i_{err,k} + \sum_{\substack{j=1\\ j\neq i}}^N \alpha^{ij}_k\mathbf{H}^T\mathbf{R}^{i|j}_k{}^{-1}\boldsymbol{\xi}^{i|j}_{err,k}$ and

$$\widehat{\mathbf{P}}^i_{k,MF} = \left(\widehat{\mathbf{P}}^i_{k|k-1,MF}{}^{-1} + \mathbf{H}^T\widehat{\mathbf{P}}^i_{nav,k}{}^{-1}\mathbf{H} + \sum_{\substack{j=1\\ j\neq i}}^N \alpha^{ij}_k\mathbf{H}^T\mathbf{R}^{i|j}_k{}^{-1}\mathbf{H}\right)^{-1}$$

where $\alpha^{ij}_k = 1$ if vehicle i receives information from vehicle j and 0 else). As the low-level filters may present divergences, it is of interest to introduce an outlier rejection procedure on the Master Filter inputs. An efficient way to reject outlying inputs is setting α_{ij} to 1 only if the input is consistent with the Master Filter estimate and predicted uncertainty. This can be done by defining an ellipsoid region to which the input measurement must belong. This ellipsoid corresponds to a given admissible covariance level on the predicted measurement provided by the Master Filter. For any available communication from vehicle j at time k:

$$\alpha^{ij}_k = \begin{cases} 1 & if\ \mathbf{y}^{i\,T}_k\widehat{\mathbf{P}}^i_{k|k-1,MF}{}^{-1}\mathbf{y}^i_k \leq \gamma_G \\ 0 & else \end{cases} \tag{16}$$

with $\mathbf{y}^i_k = \mathbf{H}\widehat{\mathbf{X}}^i_{err,k|k-1,MF} - \boldsymbol{\xi}^{i|j}_{err} \in \mathbb{R}^6$ and $\gamma_G \in \mathbb{R}^{+*}$ is obtained from a table of chi-square distribution (see Bar-Shalom [16]).

C. Comparison to a single layer fusion architecture

In this section, the proposed two layers architecture is compared with a single layer fusion, where the LOS measurements, the communicated states, and the terrain navigation measurements are fused at the same time in a BRPF. Therefore, in addition to the basic cost c_{BRPF} (10), the box contraction operation derived from (9) requires $176N_pn_m$ more elementary operations (addition, substractions, multiplications, divisions), with N_p the number of box particles and n_m the number of received communications at current time. according to the aforementioned communication strategy, $n_m = 1$. With $N_p = 900$ and $d = 15$, the single layer architecture would require 2.5×10^6 operations per time-step. Since this architecture does not require any additional filtering layer and fuses only one communicated measurement at a time, the computation load is independent from the number of vehicles N. However, it holds a high cost that can be dramatically reduced with the proposed two layers strategy.

On the basis of previous studies about filters complexity analysis [17], the proposed two layers fusion architecture computational cost can be evaluated as follows. A conventional Kalman Filter requires $c_{EKF}(d, d_m) = 4d^3 + 3d^2d_m + 2dd_m^2 + d_m^3/6$ operations, with d and d_m respectively the state dimension and the measurements dimension. Based on the same methodology, the proposed Master Filter requires $c_{MF}(d, d_m, n_m) = 4d^2 + 6d^3 + d_m^3n_m - d_m^3 + 3d_m^2n_m - 2d_m^2 - 2d + d_m$ operations. Then, the proposed architecture requires the following number of operations: $c_{total} = (N-1)c_{EKF}(d_{EKF}, d_{LOS}) + c_{BRPF}(d_{BRPF}, N_p) + c_{MF}(d_{MF}, d_{EKF}, n_m)$, with $d_{EKF} = 6$, $d_{LOS} = 3$, $d_{MF} = 15$, N the number of vehicles, and $n_m = 1$. Since the attitude and bias estimation are switched from the BRPF to the Master Filter, the BRPF dimension can be reduced

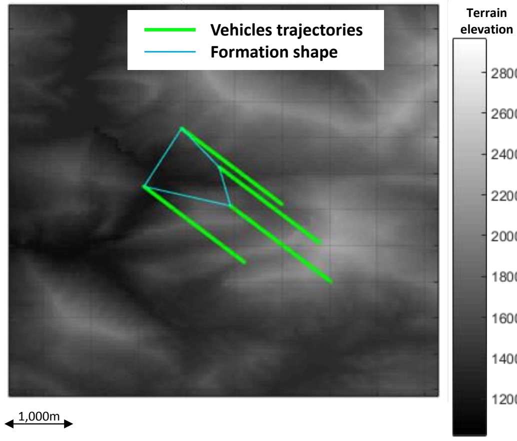

Fig. 6. UAVs trajectories (green) above a mountainous terrain (gray-scale)

to positions and velocities only ($d_{BRPF} = 6$). Therefore, the whole architecture requires a total number of operations of $1,301N + 440,163$. In the example presented in this article, with $N = 4$, the cost is of $445,367$ operations per time-step, which represents a reduction of 83.3% with respect to the single layer architecture. Theoretically, the two architectures would be equivalent in terms of computational load for $N = 1,706$ vehicles. Furthermore, the two layers architecture is theoretically more robust to relative measurements undetected outliers, since they are not introduced in any communicated data and spread through the network.

IV. NUMERICAL RESULTS

A numerical simulation is considered with four fixed-wing UAVs flying in formation over a mountainous terrain, as illustrated in Figure 6. Table I describes the simulation parameters. A hundred Monte-Carlo simulations have been run. The first evaluation criterion is the Root Mean Square Error (RMSE) defined for each agent i by $RMSE_k^i = \sqrt{\frac{1}{N_{MC}}\sum_{j=1}^{N_{MC}} \|\hat{\mathbf{x}}_{k,j} - \mathbf{x}_{k,j}\|^2}$, where $N_{MC} = 100$ is the number of runs. Vector $\hat{\mathbf{x}}_{k,j}$ stands for estimate position, velocity, or attitude at time-step k for run j. Vector $\mathbf{x}_{k,j}$ stands for actual vector to be estimated. In order to get a more general interpretation of the multi-agents estimate RMSE, one can define the global RMSE by $RMSE_k = \frac{1}{N}\sum_{i=1}^{N} RMSE_k^i$. The second evaluation criterion is the mean estimate uncertainty, defined as $\pm 3\|\widehat{\boldsymbol{\sigma}}_{\mathbf{x}}^i\|$, where $\widehat{\boldsymbol{\sigma}}_{\mathbf{x}}^i = diag\left(\widehat{\mathbf{P}}_{\mathbf{x}}^i\right)^{1/2} \in \mathbb{R}^3$ with $\widehat{\mathbf{P}}_{\mathbf{x}}^i \in \mathbb{R}^{3\times 3}$ the considered filter estimate covariance confidence of a vector $\mathbf{x} \in \mathbb{R}^3$ (position, velocity, or attitude) for agent i. A global criterion can be defined as the average value among the float: $\pm\frac{1}{N}\sum_{i=1}^{N} 3\|\widehat{\boldsymbol{\sigma}}_{\mathbf{x}}^i\|$.

Global RMSE and global estimate uncertainty are presented in Table II for the navigation BRPF, the Master Filter, and a single layer architecture that consists of a BRPF directly fusing all the measurements. The Master Filter's RMSE (159 m) remains significantly lower than the navigation BRPF (431 m) and of the same order of magnitude than the single layer architecture (145 m). As shown in Figures 7 and 8, the two layers Master Filter uncertainty ($\pm$374 m) is significantly lower than the one obtained with the navigation filter ($\pm$1,736 m), or the single layer architecture ($\pm$1,172 m). Moreover, despite the very coarse relative measurements ($\sigma_r = 500m$ for the range, which is very close to an angles-only problem), the two layers Master Filter significantly improves the velocity estimation, and performs better than the single layer estimation (4.1 m/s of RMSE with a confidence of $\pm$9.6 m/s for the Master Filter and 4.6 m/s of RMSE with a confidence of $\pm$26 m/s for the navigation filter and the single layer architecture). Attitude estimation is also enhanced with an improvement in uncertainty from $\pm 5\times 10^{-2}$ rad to $\pm 1 \times 10^{-2}$ rad. Indeed, the Information Filter converges more efficiently than a particle like filter in the case of the state variables that are not directly observed. This highlights the merits of the proposed architecture: by only measuring ground altitude and rough relative position, a complete state estimation has been performed. The additional computation time needed to perform the high-level cooperative fusion appears reasonable, since it represents an increase of only 8.4 % with respect to the low-level processing, and a computational reduction of 55 % with respect to the single layer architecture. The difference with the theoretical percentage estimated in III-C is due to the Matlab parallelization process.

TABLE I
SIMULATION CONFIGURATION

General	Value
Communication update rate	$\Delta t_{com} = 1\,\mathrm{s}$
Relative distance	10^3 m
Absolute velocity	200 m/s
IMU initial position error (std)	$[10^3, 10^3, 10^2]$ m
IMU initial velocity error (std)	$[2, 2, 1]$ m/s
IMU initial attitude error (std)	$[5\times10^{-3}, 5\times10^{-3}, 5\times10^{-3}]$ rad
IMU accelerometer bias (std)	$[10^{-2}, 10^{-2}, 10^{-2}]$ m/s^2
IMU gyrometer bias (std)	$[10^{-4}, 10^{-4}, 10^{-4}]$ rad/s
Measurements	
Radar-altimeter error (support)	$v_k \in [-45, +45]$ m
Relative angles error (std)	$\sigma_\beta = 1°$ and $\sigma_\varepsilon = 1°$
Relative range error (std)	$\sigma_r = 500\,\mathrm{m}$
Radar-altimeter update rate	$\Delta t_{RA} = 0.1\,\mathrm{s}$
Relative angles update rate	$\Delta t_\beta = 0.1\,\mathrm{s}$ and $\Delta t_\varepsilon = 0.1\,\mathrm{s}$
Relative range update rate	$\Delta t_r = 5\,\mathrm{s}$
Navigation Filter (BRPF)	$N_p = 900$, $\theta_{eff} = 0.5$
Master Filter	
Process noise in position (std)	$[80, 80, 10]$ m/s
Process noise in velocity (std)	$[2, 2, 1]$ m/s^2
Process noise in attitude (std)	$[10^{-3}, 10^{-3}, 10^{-3}]$ rad/s
Accelerometer bias (std)	$[10^{-6}, 10^{-6}, 10^{-6}]$ m/s^3
Gyrometer bias (std)	$[10^{-8}, 10^{-8}, 10^{-8}]$ rad/s^2

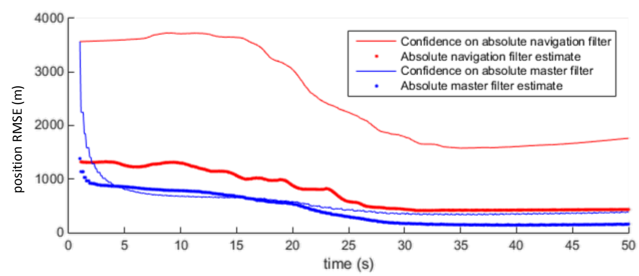

Fig. 7. Position RMSE for navigation filter and cooperative Master Filter

TABLE II
SIMULATION RESULTS AT FINAL TIME

	Navigation Filter (BRPF)	Single layer architecture (BRPF)	Two layers architecture (MF)
RMSE in position	431 m	145 m	159 m
Uncertainty in position	$\pm 1,763$ m	$\pm 1,172$ m	± 374 m
RMSE in velocity	4.6m/s	4.6m/s	4.1 m/s
Uncertainty in velocity	± 26 m/s	± 26 m/s	± 9.6 m/s
RMSE in attitude		9×10^{-3} rad	9×10^{-3} rad
Uncertainty in attitude		$\pm 5 \times 10^{-2}$ rad	$\pm 1 \times 10^{-2}$ rad
Average computation time (Desktop CPU 3.5GHz running Matlab R2014b)	8.7 ms	20 ms	9.5 ms

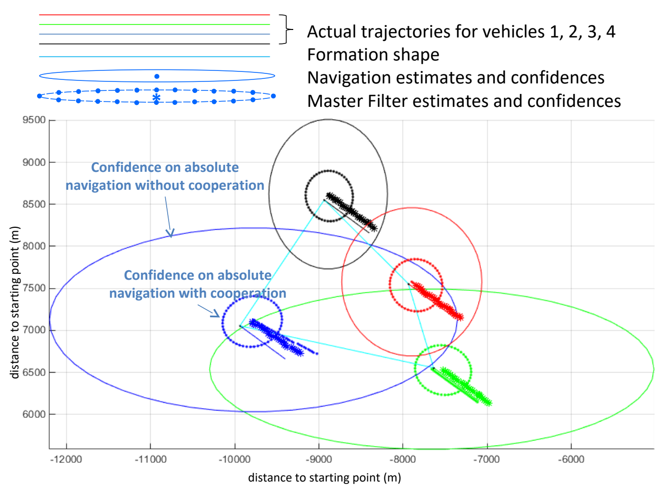

Fig. 8. Confidence estimation with cooperation (Master Filter output) and without (low-level absolute navigation filter output) for vehicles 1, 2, 3 and 4.

V. CONCLUSION

In this paper, a two-level fusion filter is presented to enable accurate absolute navigation in a GNSS denied environment for a fleet of vehicles. The fusion architecture consists of two low-level filters and a high-level Master Filter. A Box Regularized Particle Filter provides an initial estimate of the navigation solution using a terrain navigation technique. Relative navigation is performed by an EKF. An information filter fuses those two filters' outputs with communicated navigation information from neighbors. The resulting filter makes it possible to enhance IMU error estimation from incomplete and ambiguous measurements, such as ground altitude data and roughly estimated relative states. This approach offers the advantage of being computationally lighter than a single layer BRPF, and does not introduce any hierarchy between vehicles, since each one broadcasts its state and uses other vehicles communicated information, if available and consistent. The use of IMU errors makes it possible to rely on a linear dynamical model, independent from the vehicle dynamical model. Therefore, the proposed approach does not require any simplification or assumption about the vehicle dynamics, contrary to many collaborative localization approaches. Another advantage is that most approaches assume availability of accurate navigation sensors, such as GNSS receivers, or are limited to partial state vector estimation. The use of fused Box Regularized Particle Filters makes it possible to accurately correct each IMU error using very coarse measurements. From a measured altitude above the ground and inaccurate relative measurements, a complete navigation solution for the whole state vector is proposed. Significant improvements, both in accuracy and predicted uncertainty, have been shown, compared to the use of the low level absolute navigation filter alone, or a single layer architecture.

REFERENCES

[1] Y. Wu, R. Lu, P. Shi, H. Su, and Z.-G. Wu, "Adaptive output synchronization of heterogeneous network with an uncertain leader," *Automatica*, vol. 76, pp. 183–192, 2017.
[2] K. Dahia, "Nouvelles méthodes en filtrage particulaire-application au recalage de navigation inertielle par mesures altimétriques," Ph.D. dissertation, Université Joseph-Fourier-Grenoble I, 2005.
[3] N. Merlinge, K. Dahia, and H. Piet-Lahanier, "A box regularized particle filter for terrain navigation with highly non-linear measurements," *Proceeding of the IFAC ACA Conference*, vol. 49, no. 17, pp. 361–366, 2016.
[4] A. Gning, B. Ristic, L. Mihaylova, and F. Abdallah, "An introduction to box particle filtering," *IEEE Signal Processing Magazine*, pp. 166–171, 2013.
[5] C. Musso, N. Oudjane, and F. LeGland, "Improving regularized particle filters," *Sequential Monte Carlo Methods in Practice*, vol. 12, pp. 247–271, 2001.
[6] R. Sharma and C. Taylor, "Cooperative navigation of mavs in gps denied areas," in *IEEE International Conference on Multisensor Fusion and Integration for Intelligent Systems*. IEEE, 2008, pp. 481–486.
[7] H. Li and F. Nashashibi, "Cooperative multi-vehicle localization using split covariance intersection filter," *IEEE Intelligent transportation systems magazine*, vol. 5, no. 2, pp. 33–44, 2013.
[8] S.-L. Sun and Z.-L. Deng, "Multi-sensor optimal information fusion kalman filter," *Automatica*, vol. 40, no. 6, pp. 1017–1023, 2004.
[9] X. Wang, N. Cui, and J. Guo, "Ins/visnav/gps relative navigation system for uav," *Aerospace Science and Technology*, vol. 28, no. 1, pp. 242–248, 2013.
[10] N. A. Carlson, "Federated square root filter for decentralized parallel processors," *IEEE Transactions on Aerospace and Electronic Systems*, vol. 26, no. 3, pp. 517–525, 1990.
[11] R. Moore, F. Bierbaum, and K. Schwiertz, *Methods and Applications of Interval Analysis*. Philadelphia: SIAM, 1979.
[12] R. Karlsson, T. Schon, and F. Gustafsson, "Complexity analysis of the marginalized particle filter," *IEEE Transactions on Signal Processing*, vol. 53, no. 11, pp. 4408–4411, 2005.
[13] S. Leung and O. Montenbruck, "Real-time navigation of formation-flying spacecraft using global-positioning-system measurements," *Journal of Guidance, Control, and Dynamics*, vol. 28, no. 2, pp. 226–235, 2005.
[14] N. Oudjane, "Stabilité et approximations particulaires en filtrage non linéaire application au pistage," Ph.D. dissertation, Université de Rennes, 2000.
[15] B. Grocholsky, "Information-theoretic control of multiple sensor platforms," Ph.D. dissertation, University of Sydney. School of Aerospace, Mechanical and Mechatronic Engineering, 2002.
[16] Y. Bar-Shalom, P. K. Willett, and X. Tian, *Tracking and data fusion*. YBS publishing, 2011.
[17] M. Verhaegen and P. Van Dooren, "Numerical aspects of different kalman filter implementations," *IEEE Transactions on Automatic Control*, vol. 31, no. 10, pp. 907–917, 1986.